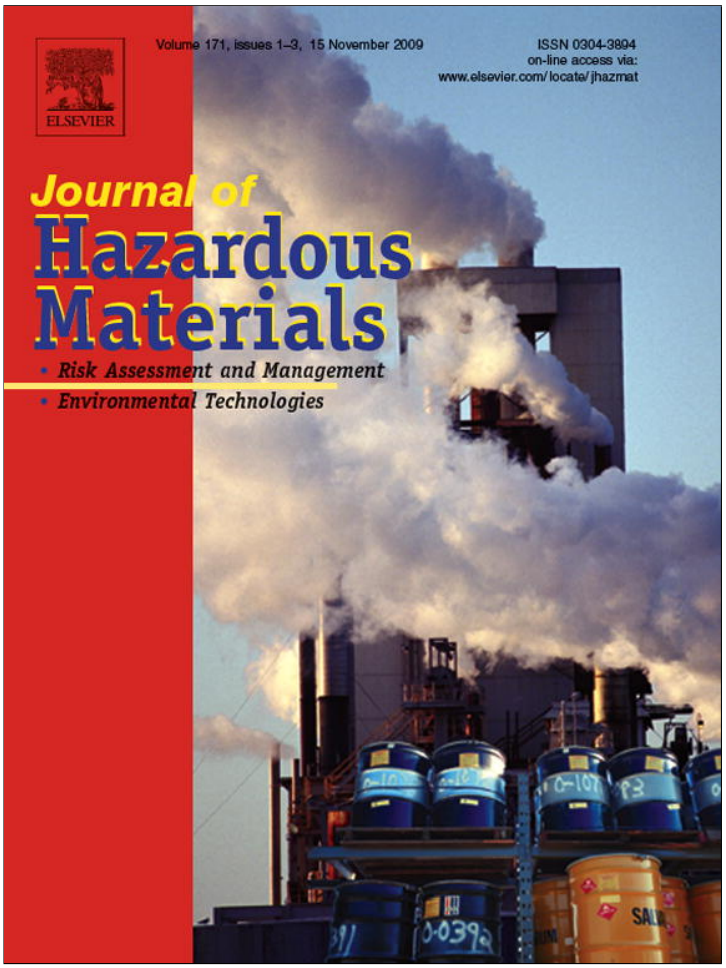

Journal of Hazardous Materials 171 (2009) 1032–1044

Contents lists available at ScienceDirect

Journal of Hazardous Materials

journal homepage: www.elsevier.com/locate/jhazmat

Degradation pathways of crystal violet by Fenton and Fenton-like systems: Condition optimization and intermediate separation and identification

Huan-Jung Fan[b], Shiuh-Tsuen Huang[a], Wen-Hsin Chung[c], Jeng-Lyan Jan[b], Wan-Yu Lin[c], Chiing-Chang Chen[a,*]

[a] Department of Science Application and Dissemination, National Taichung University, Taichung 403, Taiwan, ROC
[b] Department of Environmental Engineering, Hungkuang University, Taichung 433, Taiwan, ROC
[c] Department of Plant Pathology, National Chung Hsing University, Taichung 402, Taiwan, ROC

ARTICLE INFO

Article history:
Received 17 December 2008
Received in revised form 19 June 2009
Accepted 19 June 2009
Available online 27 June 2009

Keywords:
Fenton
Fenton-like
Crystal violet
N-de-methylation

ABSTRACT

The main advantage of Fenton's reagent (FR) over other •OH systems is its simplicity. FR has the potential for widespread use in treating wastewater, but compared to other •OH systems, little information on the dye degradation pathways of FR exists. The degradation of crystal violet (CV), a triphenylmethane dye, by FR was determined as a function of reagent concentration and ratio and pH in the batch treatment. The experimental results showed the optimum Fe^{2+}/H_2O_2 ratio to be 0.5 mM:50 mM and the optimum Fe^{3+}/H_2O_2 ratio to be 1 mM:50 mM. Optimal pH was about 3. To obtain a better understanding of the mechanistic details of Fenton reagent's degradation of CV dye, the intermediates of the process were separated, identified, and characterized by HPLC–PDA-ESI-MS and GC–MS techniques in this study. Indications were that the probable degradation pathways were *N*-de-methylation and cleavage of the conjugated chromophore structure. The intermediates were generated in the order of the reaction time and relative concentration, indicating that the *N*-de-methylation degradation of CV dye is a major reaction pathway. The reaction mechanisms proposed in this research should prove useful for future application of the technology to the decolorization of dyes.

1. Introduction

In 1894 Fenton reported that alcohols are oxidized in the presence of H_2O_2 and $Fe(H_2O)_6{}^{2+}$ [1]. As shown in Eq. (1), the reaction produces strong oxidative hydroxyl radicals, and the ferrous ions are oxidized to ferric ions. Since, both ferrous and ferric ions are coagulants, the Fenton process can therefore perform the dual functions of oxidation and coagulation in the treatment process. In the past few decades, the Fenton process has been used to treat recalcitrant/toxic wastewaters [2–4] and decolorize dyes [5–7]. The Fenton reaction has proven effective at treating organic pollutants in wastewater, and the mechanism and kinetics have been studied by many researchers [8–15]. In classic Fenton chemistry, the reaction between hydrogen peroxide and Fe^{2+} in an acidic aqueous solution is generally recognized to produce hydroxyl radicals (Eq. (1)) and can involve the reactions presented below (Eqs. (1)–(6)). The generally accepted free radical chain mechanism for the Fenton reaction is shown below [8,16–19], and the slow reaction (Eq. (2)) is the rate-determining step. The rate constants are reported at 298 K in $M^{-1}\,s^{-1}$ for a second-order reaction rate [20,21].

$$Fe^{2+} + H_2O_2 \rightarrow Fe^{3+} + {}^{\bullet}OH + OH^- \quad k_1 = 63 \tag{1}$$

$$Fe^{3+} + H_2O_2 \rightarrow Fe^{2+} + HO_2{}^{\bullet} + H^+ \quad k_2 = 0.002\text{–}0.01 \tag{2}$$

$$Fe^{2+} + {}^{\bullet}OH \rightarrow Fe^{3+} + OH^- \quad k_3 = 3 \times 10^8 \tag{3}$$

$$H_2O_2 + {}^{\bullet}OH \rightarrow HO_2{}^{\bullet} + H_2O \quad k_4 = 2.7 \times 10^7 \tag{4}$$

$$Fe^{2+} + HO_2{}^{\bullet} \rightarrow Fe^{3+} + HO_2{}^- \quad k_5 = 1.2 \times 10^6 \tag{5}$$

$$Fe^{3+} + HO_2{}^{\bullet} \rightarrow Fe^{2+} + H^+ + O_2 \quad k_6 < 2 \times 10^3 \tag{6}$$

The free radical mechanism of the Fenton reaction has been questioned from time to time, and alternatives have been proposed that involve hypothetical transients other than free •OH [1,22,23]. In recent years, researchers have firmly established that complexes of Fe^{2+} and/or Fe^{3+} with organic ligands may react with peroxides, dioxygen, or other oxidants to form a high-valent oxoiron moiety, Fe=O, where iron is formally in the +IV or +V oxidation state [24,25]. Such reactions may generate •OH concurrently, a result that has confounded the interpretation of some experiments. The ferryl poiety can oxidize organic compounds, and there is general agreement that it participates in both the oxygen atom and electron-transfer reactions of many heme and

* Corresponding author. Tel.: +886 4 22183839; fax: +886 4 22183530.
E-mail address: ccchen@mail.ntcu.edu.tw (C.-C. Chen).

0304-3894/$ – see front matter © 2009 Elsevier B.V. All rights reserved.
doi:10.1016/j.jhazmat.2009.06.117

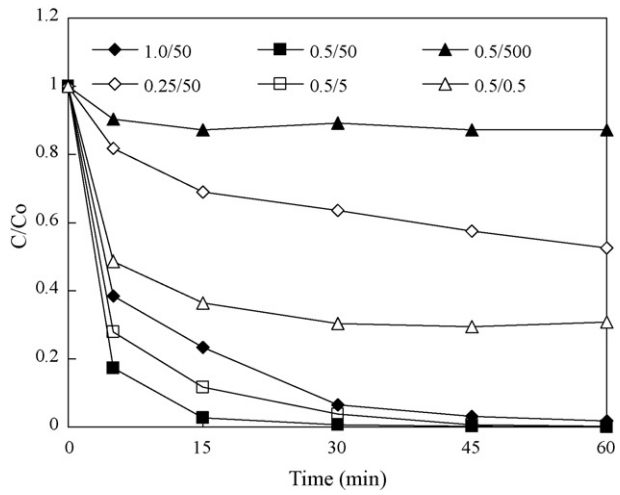

Fig. 1. Effect of $[Fe^{2+}]/[H_2O_2]$ molar ratio on the degradation of CV dye during oxidation treatment. Reaction conditions: $[CV]_o = 0.15$ mM, pH 5.

nonheme enzymes [24,25]. Other forms of "active oxygen" in reactions of hydrogen peroxide with complexed iron in organic solvents have been suggested [26]. Yamazaki and Piette [27] observed three types of oxidizing species (free hydroxyl radical, bound hydroxyl radical, and high-valence iron species, which is probably a ferryl ion, FeO^{4+}) using EPR spin trapping. Kremer [28] hypothesized the formation of "FeO^{3+}" in dark Fe^{3+}/H_2O_2 reactions, and Ensing et al. [29] reported the formation $Fe^{III}HO_2{}^{2+}$ in Fe^{3+}/H_2O_2 systems. Earlier reports, publishing mainly the relative reactivities of the intermediate of the original Fenton reaction toward various substrates and comparing them to those of hydroxyl radicals produced by radiation chemistry, established that the data are essentially in agreement with the •OH radical being the active intermediate, unless ferryl species and •OH radicals are kinetically equivalent [8]. However, more recent findings demonstrate discrepancies in reactivity patterns when an extensive list of substrates is studied and when there are two active intermediates (presumably a ferryl species and iron-peroxo complex) that differ from the radical [30]. This reaction mechanism, however, is still a subject of debate.

Around 10^6 tons and more than 10,000 different synthetic dyes and pigments are produced annually worldwide, and these are used extensively in the dye and printing industries. It is estimated

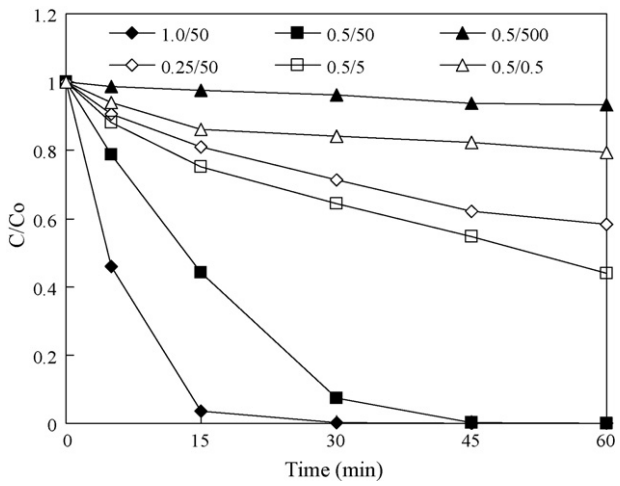

Fig. 2. Effect of $[Fe^{3+}]/[H_2O_2]$ molar ratio on the degradation of CV dye during oxidation treatment. Reaction conditions: $[CV]_o = 0.15$ mM, pH 5.

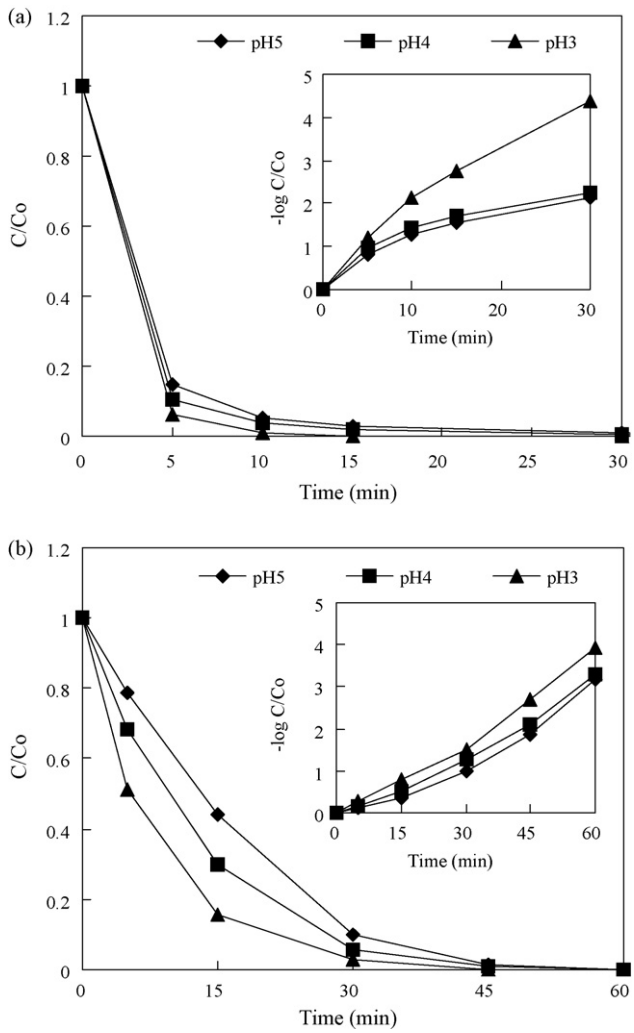

Fig. 3. Effect of pH on the degradation of CV dye during (a) Fenton and (b) Fenton-like oxidation treatment. Reaction conditions: $[CV]_o = 0.15$ mM, $[Fe^{2+}]$, $[Fe^{3+}] = 0.5$ mM, and $[H_2O_2] = 50$ mM.

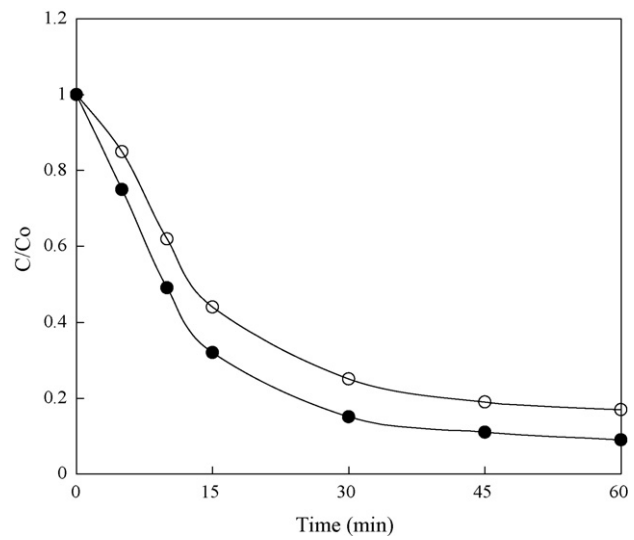

Fig. 4. Depletion in TOC as a function of reaction time for an aqueous solution of CV in the presence of Fenton and Fenton-like reagent at pH 5. Experimental conditions: CV dye concentration (0.15 mM), $[Fe^{2+}]$, $[Fe^{3+}] = 0.5$ mM, and $[H_2O_2] = 50$ mM, continuous stirring, and reaction time 60 min.

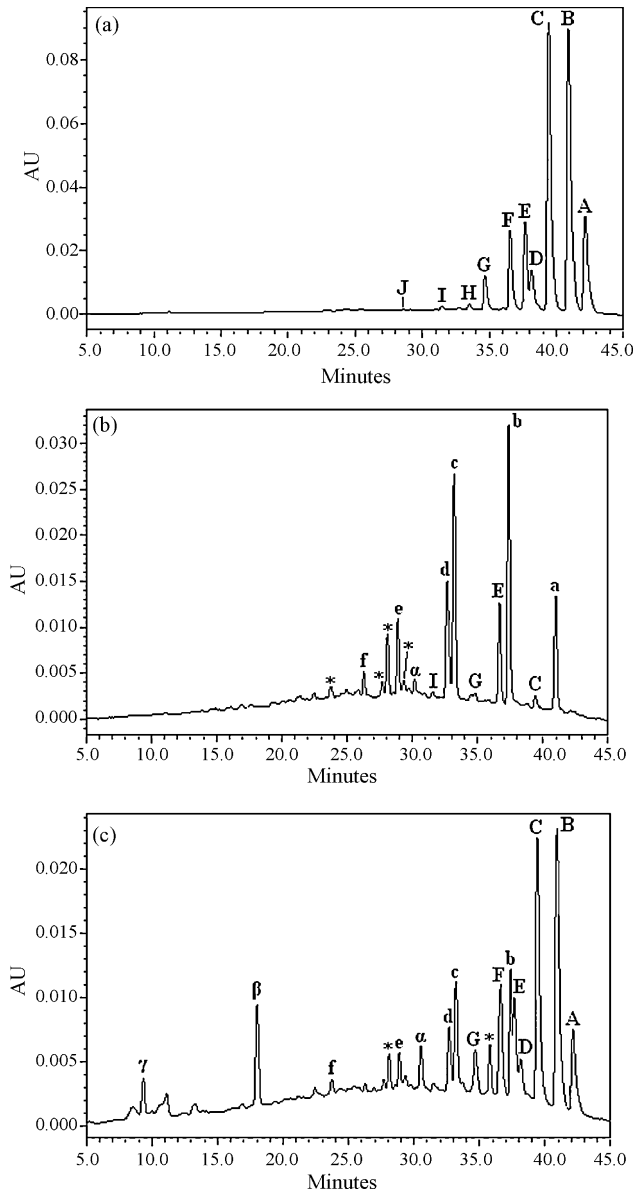

Fig. 5. HPLC chromatogram of the intermediates with 30 min of Fenton reaction at pH 5, recorded at (a) 580 nm, (b) 350 nm, and (c) 300 nm.

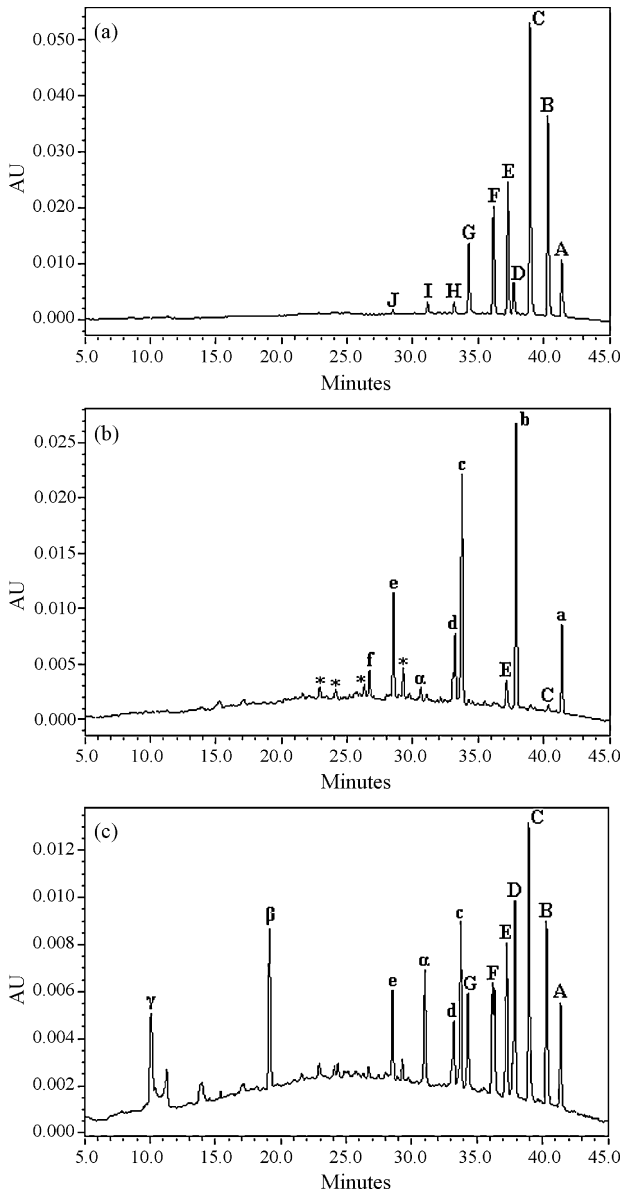

Fig. 6. HPLC chromatogram of the intermediates with 30 min of Fenton-like reaction at pH 5, recorded at (a) 580 nm, (b) 350 nm, and (c) 300 nm.

that about 10% are lost in industrial effluents [31]. Triphenylmethane (TPM) dyes are suitable for a large variety of technological applications. They are used extensively in the textile industry for dyeing nylon, wool, cotton, and silk, as well as for coloring oil, fats, waxes, varnish, and plastics. The paper, leather, cosmetic, and food industries are other major consumers of various TPM dyes [32,33]. Cationic TPM dyes are widely used as antimicrobial agents [33]. Recent reports indicate that they may further serve as targetable sensitizers in the photodestruction of specific cellular components or cells [34,35]. Additionally, the TPM dyes are applied as staining agents in bacteriological and histopathological applications. The photocytotoxicity of TPM dyes based on reactive oxygen species production has been tested intensively with a view to developing a photodynamic therapy [36]. However, the thyroid peroxidase-catalyzed oxidation of the TPM class of dyes is of great concern because the reactions might form various *N*-de-alkylated primary and secondary aromatic amines, with structures similar to aromatic amine carcinogens [35].

Environmental pressures have impelled the search for new technological developments. CV has been studied in several hydroxyl radical (•OH) generating systems, including TiO_2/UV or VIS (37–38), ZnO/UV [39], H_2O_2/UV [40], Fe^{2+}/H_2O_2/UV [40] and Fe^{3+}/UV [41]. In most cases, reaction mechanisms, kinetics, and/or efficiency are well documented, but the FR reaction mechanism is still a subject of debate. According to the classical interpretation, the active oxidizing species degrading organic matter are •OH radicals. Therefore, the main advantage of Fenton's reagent over other •OH systems is simplicity: the chemicals are commonly available and inexpensive, and special equipment like UV lamps, complex reaction vessels, TiO_2/ZnO particles, or ozone generators is unnecessary. Because of this simplicity, FR has the potential for widespread use in treating dye wastes. However, compared to other •OH systems, little information exists on dye degradation by FR. The degradation intermediates of this CV have not been isolated or identified by HPLC–ESI-MS or GC–MS techniques in the Fenton process. The mechanistic details of degradation remain uncertain.

This study is aimed at understanding the intermediates and mechanisms of oxidation of CV dye in the Fenton process. The role of some conditions such as pH, initial [H_2O_2] and [Fe^{2+}], and initial [H_2O_2] and [Fe^{3+}] were examined in order to provide a full description of this system.

2. Experimental

2.1. Materials and reagents

Chloride salt of crystal violet (CV; CI 42555; Basic Violet 3; hexamethylpararosaniline chloride; Methyl Violet 10B) was obtained from Tokyo Kasei Kogyo Co., and HPLC analysis confirmed that the CV was a pure organic compound. Stock solutions containing 2.69 mM (1000 mg/L) of CV in aqueous solution were prepared, protected from light, and stored at 4 °C. $FeSO_4{\cdot}7H_2O$ and $Fe(NO_3)_3{\cdot}9H_2O$ were purchased from Hayashi, and H_2O_2 (35% solution) was from Shimakyu. Reagent-grade ammonium acetate, nitric acid, sodium hydroxide, and HPLC-grade methanol were purchased from Merck. De-ionized water was used throughout this study. The water was purified with a Milli-Q water ion-exchange system (Millipore Co.) until it gave a resistivity of 1.8×10^7 Ω-cm.

2.2. Instruments

A Waters ZQ LC/MS system – equipped with a Waters 1525 Binary HPLC pump, a Waters 2996 Photodiode Array Detector, a Waters 717plus Autosampler, and a Waters micromass-ZQ4000 Detector – was used to identify the reaction intermediates. GC/MS analyses were run on a Perkin-Elmer AutoSystem-XL gas chromatograph interfaced to a TurboMass selective mass detector.

2.3. Experiments

The Fe^{2+} or Fe^{3+} Fenton's catalyst stock solution consisted of 5 mM $FeSO_4{\cdot}7H_2O$ or $Fe(NO_3)_3{\cdot}9H_2O$. In addition, a [Fe^{2+}] or [Fe^{3+}] Fenton's catalyst was prepared by diluting stock solution in de-ionized water, followed by pH adjustment to 3–5 with 0.1 M HCl. Ratios ($FeSO_4$:H_2O_2 or $Fe(NO_3)_3$:H_2O_2) of 0.25:50, 0.5:50, 1.0:50, 0.5:0.5, 0.5:5, 0.5:50, and 0.5:500 (mM) were examined. Solutions of $FeSO_4$ or $Fe(NO_3)_3$ (0.25–1.0 mM) and CV dye (0.15 mM) were mixed in 100 mL flasks, and •OH production was initiated by adding 0.5–500 mM H_2O_2. Samples (0.5 mL) were mixed with methanol (0.5 mL) to quench the reaction and centrifuged (10 min; 3200 rpm), and the supernatants were analyzed by HPLC–PDA-ESI-MS and GC–MS.

2.4. Procedures and analyses

The amount of residual dye at each reaction cycle was determined by HPLC–PDA-ESI-MS. The analysis of organic intermediates was accomplished by HPLC–PDA-ESI-MS after readjustment of chromatographic conditions in order to make the mobile phase (Solvent A and B) compatible with the working conditions of the mass spectrometer. Solvent A was 25 mM aqueous ammonium acetate buffer (pH 6.9), and solvent B was methanol. LC was carried out on an Atlantis™ dC18 column (250 mm × 4.6 mm i.d., dp = 5 μm). The mobile phase flow rate was 1.0 mL/min. A linear gradient was run as follows: $t = 0$, $A = 95$, $B = 5$; $t = 20$, $A = 50$, $B = 50$; $t = 35$–40, $A = 10$, $B = 90$; $t = 45$, $A = 95$, $B = 5$. The column effluent was introduced into the ESI source of the mass spectrometer. The quadruple mass spectrometer equipped with an ESI interface with heated nebulizer probe at 350 °C was used with an ion source temperature of 80 °C. ESI was carried out with the vaporizer at 350 °C and nitrogen as sheath (80 psi) and auxiliary (20 psi) gas to assist

Table 1
The degraded intermediates of CV by Fenton process.

HPLC peaks	Intermediates	ESI-MS spectrum ions (*m*/*z*)	Absorption maximum (nm)
A	*N*,*N*,*N*′,*N*′,*N*″,*N*″-hexaethylpararosaniline	372.18	588.2
B	*N*,*N*-dimethyl-*N*′,*N*′-dimethyl-*N*″-methyl pararosaniline	358.14	581.1
C	*N*,*N*-dimethyl-*N*′-methyl-*N*″-methylpararosaniline	344.10	573.4
D	*N*,*N*-dimethyl-*N*′,*N*′-dimethyl pararosaniline	344.09	579.5
E	*N*-methyl-*N*′-methyl-*N*″-methyl pararosaniline	330.10	566.1
F	*N*,*N*-dimethyl-*N*′-methylpararosaniline	330.36	570.7
G	*N*-methyl-*N*′-methylpararosaniline	316.15	561.8
H	*N*,*N*-dimethylpararosaniline	316.17	566.2
I	*N*-methylpararosaniline	302.06	554.1
J	Pararosaniline	288.07	543.4
a	4-(*N*,*N*-dimethylamino)-4′-(*N*′,*N*′-dimethylamino)benzophenone	269.05	376.4
b	4-(*N*,*N*-dimethylamino)-4′-(*N*′-methylamino)benzophenone	255.06	366.6
c	4-(*N*-methylamino)-4′-(*N*′-methylamino)benzophenone	240.92	364.4
d	4-(*N*,*N*-dimethylamino)-4′-aminobenzophenone	240.98	358.8
e	4-(*N*-methylamino)-4′-aminobenzophenone	226.84	357.3
f	4,4′-Bis-aminobenzophenone	213.06	337.5
α	4-(*N*,*N*-dimethylamino)phenol	138.16	309.7
β	4-(*N*-methylamino)phenol	124.03	283.6
γ	4-aminophenol	110.14	278.1

GC peaks	Intermediates	EI-MS spectrum ions (*m*/*z*)
a′	4-dimethylaminobenzoic acid	N/A
b′	4-methylaminobenzoic acid	N/A
c′	4-aminobenzoic acid	N/A
a″	*N*,*N*-dimethylaminobenzene	N/A
b″	*N*-methylaminobenzene	107, 106, 77, 51[a]
c″	Aminobenzene	93, 66[a]
I	1-hydroxy-2-propanone	74, 43, 31, 15[a]
II	Acetic acid	60, 45, 43, 15[a]

The other intermediates were identified by HPLC–ESI-MS.
[a] The intermediates were identified by GC–MS.

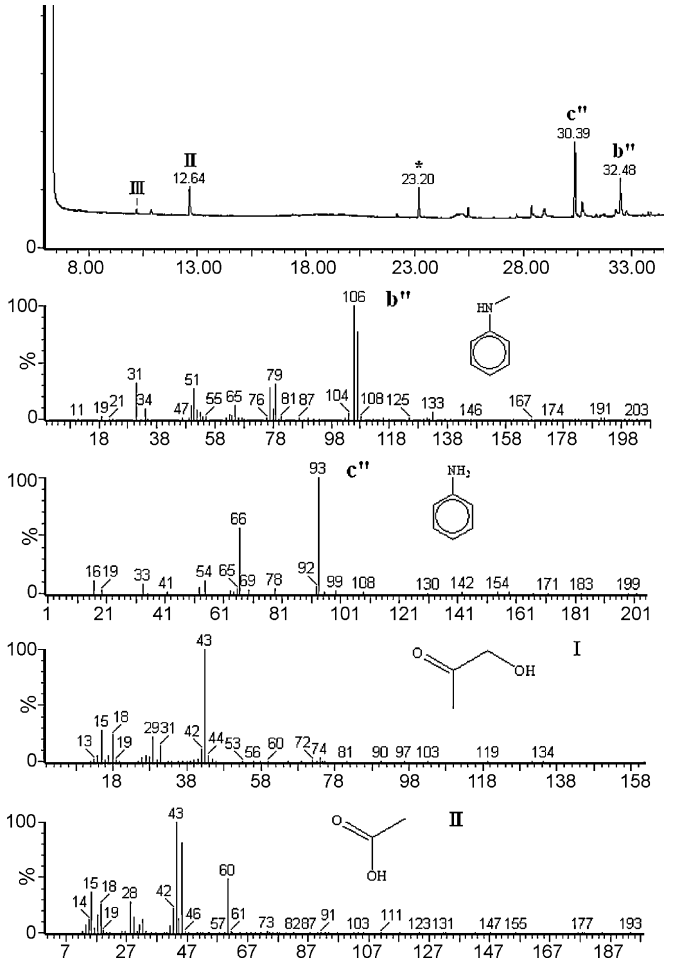

Fig. 7. GC–MS/EI chromatogram obtained for a SPE extract of CV solution after 60 min of Fenton oxidation.

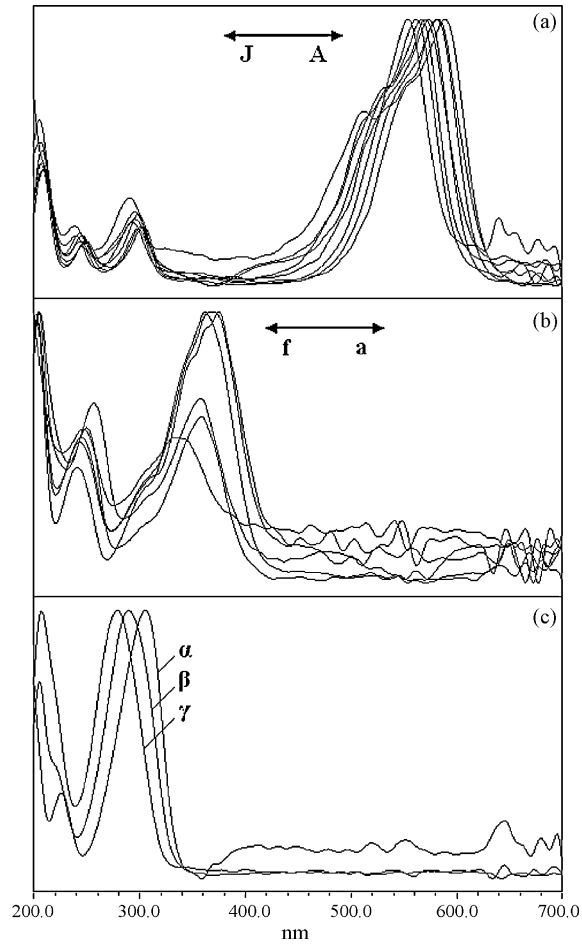

Fig. 8. Absorption spectra of the intermediates formed during the Fenton process of the CV dye corresponding to the peaks in the HPLC chromatograph of Fig. 6. Spectra were recorded using the photodiode array detector. (a) Spectra A–J, (b) a–f, and (c) α–γ correspond to the peaks A–J, a–f, and α–γ, respectively, in Fig. 6.

with the preliminary nebulization and to initiate the ionization process. A discharge current of 5 μA was applied. Tube lens and capillary voltages were optimized for maximum response during perfusion of the CV standard.

Solid-phase extraction (SPE) was employed for preconcentration of irradiated samples prior to GC/MS analysis. Oasis HLB (hydrophilic/lipophilic balance) was used as the sorbent to ensure good recovery of compounds in a wide range of polarities. The cartridges were placed in a vacuum cube (provided by Supelco) and conditioned with 5 mL of methanol and 5 mL of de-ionized water. After the conditioning step, 100 mL aliquots of the samples were loaded at a flow rate of approximately 10 mL/min. Elution was performed with 8 mL of methanol. The eluates obtained were concentrated by solvent evaporation with a gentle nitrogen stream and recomposed to a final volume of 1 mL in methanol. The extracts were stored in amber vials and refrigerated until chromatographic analysis to prevent further degradation.

GC/MS analyses were carried out in a DB-5 capillary column (5% diphenyl/95% dimethyl-siloxane), 60 m, 0.25-mm i.d., and 1.0-μm thick film. A split-splitless injector was used under the following conditions: injection volume 1 μL, injector temperature 280 °C, split flow 10 mL/min. The helium carrier gas flow was 1 mL/min. The oven temperature program was 4.0 min at 40 °C, 4 °C/min to 80 °C (2 min), 8 °C/min to 280 °C (9 min). Electron impact (EI) mass spectra were monitored from 10 to 300 *m/z*. The ion source and inlet line temperatures were set at 220 and 280 °C, respectively.

Blank experiments performed in flask with H_2O_2 showed no appreciable decolorization of the solution, thus confirming the expected good stability of this CV dye under our conditions.

3. Results and discussion

3.1. Fenton's and Fenton-like system

3.1.1. Effect of $[Fe^{2+}]/[H_2O_2]$ concentration ratio on degradation of dye

The experimental results indicated that CV could be degraded efficiently in solution by Fenton (Fe^{2+}/H_2O_2) (Fig. 1). Fig. 1 shows that the CV dye underwent a 97% decolorization after 15 min of reaction time under experimental conditions (Fe^{2+} 0.5 mM, H_2O_2 50 mM, pH 5). However, an increased Fe^{2+} concentration from 0.5 mM to 1.0 mM induced a decreased rate of CV degradation, and a roughly 76% decrease in color was observed (Fig. 1). This can be explained by the fact that the very reactive •OH radical could be consumed by Fe^{2+}, and subsequently by Fe^{3+}, which is necessary to form peroxide radicals (HO_2•). Therefore, a dramatic reduction in oxidation efficiency is expected. Moreover, many studies have revealed that the use of a much higher Fe^{2+} concentration could lead to the self-scavenging of •OH radical by Fe^{2+} (Eq. (3)) [20,21] and induce the decrease in the degradation rate of pollutants.

Generally speaking, an increase in the H_2O_2 concentrations was the first positive for the degradation of CV. This is due to the oxidation power of the Fenton system, which improved with increasing

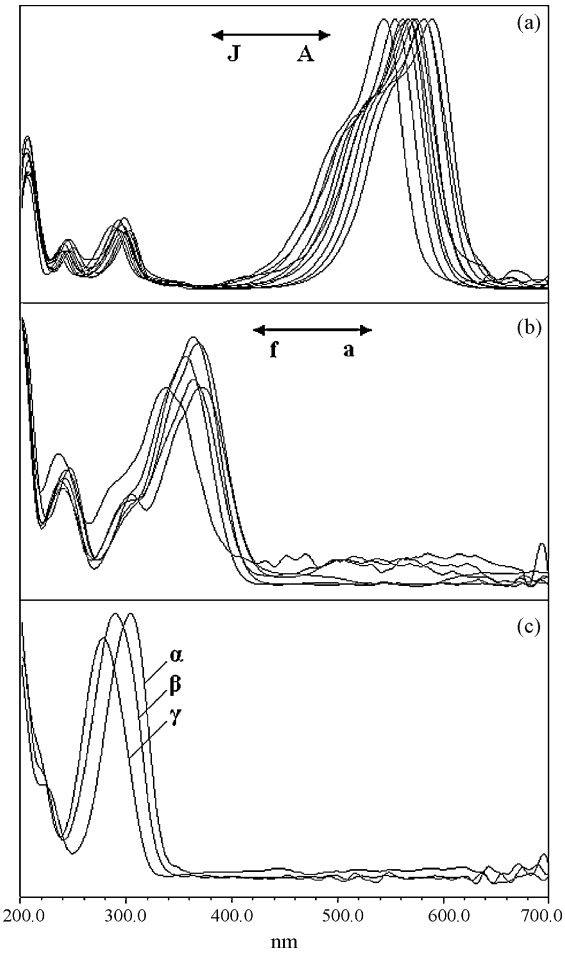

Fig. 9. Absorption spectra of the intermediates formed during the Fenton-like process of the CV dye corresponding to the peaks in the HPLC chromatograph of Fig. 6. Spectra were recorded using the photodiode array detector. (a) Spectra A–J, (b) a–f, and (c) α–γ correspond to the peaks A–J, a–f, and α–γ, respectively, in Fig. 6.

•OH radical amounts in the solution obtained from increasing H_2O_2 concentrations. Fig. 1 shows the continuous increase of H_2O_2 to 500 mM. The CV degradation rate fell. This may be explained by the fact that the very reactive •OH radical can be consumed by H_2O_2, which results in the generation of less reactive HO_2• radicals (Eq. (4)) [20,21]. In the following experiment, we chose a $[Fe^{2+}]/[H_2O_2]$ concentration ratio of 0.5/50 (mM) as optimum.

3.1.2. Effect of $[Fe^{3+}]/[H_2O_2]$ concentration ratio on dye degradation

The main process variables affecting the rate of a Fenton-like reaction are the molar concentrations of the oxidant (H_2O_2) and catalyst (Fe^{3+}), particularly the Fe^{3+}:H_2O_2 molar ratio. The experimental results showed that the optimum Fe^{3+}:H_2O_2 molar ratio for the removal of CV was 1:50 (Fig. 2). At 15 min into the reaction, dye removal was about 96% under pH 5. It is known from studies available on the production of •OH radical that the number of cyclic reactions (Eqs. (1) and (2)) has a considerable effect on the oxidation of CV. The reaction of Fe^{3+} with H_2O_2 leads to the formation of Fe^{2+} ions, which can further react with H_2O_2 to produce OH radical. Therefore, a low Fe^{3+} concentration decreases CV degradation. CV removal actually ceased when the Fe^{3+}:H_2O_2 molar ratio increased from 1:50 to 1:500 for 1 mM Fe^{3+}, indicating that H_2O_2 was overdosed when its concentration rose tenfold (Fig. 2). In the presence 50 mM of H_2O_2, the ionic liquid is probably eliminated solely by the reaction with •OH, but at 500 mM, additional quenching by H_2O_2 also occurs. Furthermore, the oxidation of ionic liquids – not only by reaction with •OH radicals, but also by other radical species generated in vigorous Fe^{+3}/H_2O_2 reactions such FeO^{3+} [28], and $Fe^{III}HO_2^{2+}$ [29] – then decrease •OH radical production. Similar phenomena were reported for the degradation of 1-butyl-3-methylimidazolium chloride [42]. This is due to the fact that degradations in modified Fenton systems have been interpreted as oxidation by •OH radicals. Nevertheless, one has to be aware that the studied oxidation system might be of much greater complexity. In the following experiment, we chose a $[Fe^{3+}]/[H_2O_2]$ concentration ratio of 1/50 (mM) as optimum.

3.1.3. Effect of pH on Fenton and Fenton-like reactions

The oxidation of CV as a function of pH is shown in Fig. 3. It is evident that a change in the pH of the solution to a Fenton and Fenton-like value of 3 leads to increases in the extent of CV oxidation. The decrease in oxidation rate at pH > 3 could be explained by the formation of $Fe(OH)_3$, which has lower catalytic activity in the decomposition of H_2O_2 [43]. At pH < 3, CV dye easily forms leuco CV [44]. However, this paper demonstrates that the pH value for the most effective oxidation of CV is approximately 3. The results closely agreed with those in the literature [13], which found the optimum pH of Safranine T oxidation using the classic Fenton's reagent was 3. Lu et al. [45] also found that the optimum pH of dichlorvos oxidation using Fenton's reagent was between 3 and 4. They also found that the rate of oxidation decreased when the solution pH was 2.5. The lower efficiency at pH 2.5 is probably due to the formation of the complex species $[Fe^{(II)}(H_2O)_6]^{2+}$, which reacts more slowly with H_2O_2 than $[Fe^{(II)}(OH)(H_2O)_5]^{+}$, and therefore produces fewer •OH radicals [46]. Additionally, at a very low pH, the reaction of Fe^{3+} with H_2O_2 is inhibited [47,48], and •OH is scavenged by H^+ [49].

3.1.4. Evolution of TOC

The complete mineralization of 1 mol CV dye molecule implies the formation of the equivalent amount (25 moles) of CO_3^{2-} at the end of the treatment. However, the depletion in TOC (shown in Fig. 4) clearly indicates that the reaction does not go to completion. In fact, after 60 min of reaction, about 91.9% of the initial organic carbon had been transformed into CO_2, which implied the existence of other organic compounds in the solution. This is supported by the HPLC–PDA-ESI-MS analysis, which suggests the presence of residual organic products even after 60 min of reaction, confirming the noticeable degradation of the examined dye.

3.2. Separation and identification of the intermediates

3.2.1. LC–MS techniques

The behavior of the aromatic intermediates formed during the mineralization of CV dye by Fenton and Fenton-like oxidation is shown in Figs. 5 and 6. The reaction intermediates were examined by HPLC using a photodiode array detector and ESI mass spectrometry. The results of HPLC chromatograms, UV–visible spectra, and HPLC–ESI mass spectra are summarized in Table 1. The nineteen intermediates were identified and all had retention times under 45 min. The chromatograms at pH 5 are identified as peaks **A–J**, **a–f**, and **α–γ** in Fig. 5(a–c) and were recorded at 580, 350, and 300 nm, respectively. This was similar to the results observed in Fenton-like reactions Fig. 6(a–c). Except for the initial CV dye (peak **A**), the rest of the peaks appear at the end of the 30-min of reaction, indicating formation and transformation of intermediates.

3.2.2. GC–MS techniques

The GC–MS analysis of the Fenton system of a CV solution showed the formation of several final products, four of which

have been identified based on their molecular ion and mass spectrometric fragmentation peaks, which are shown in Fig. 7. The experimental conditions were Fe^{2+} 0.5 mM, H_2O_2 50 mM, and a 60-min reaction at pH 5. GC–EI chromatograms identified peaks **b**′′, **c**′′, **I**, and **II**, and mass spectra are summarized in Table 1.

3.3. Identification of the intermediates

3.3.1. UV–visible spectra of intermediates in Fenton and Fenton-like systems

The absorption spectra of each intermediate in the absorption spectral region are measured corresponding to the peaks in Fig. 8.

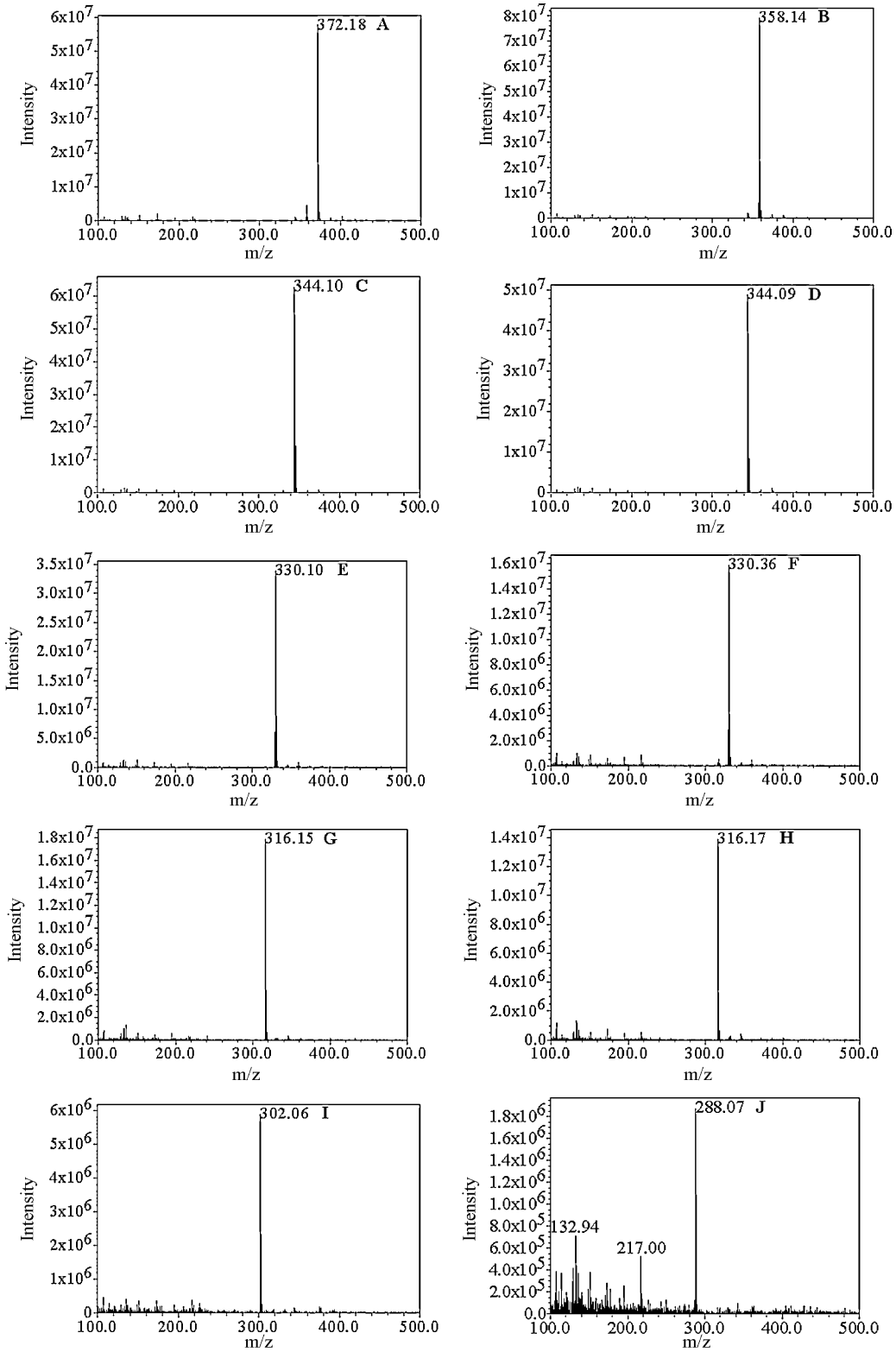

Fig. 10. (**A–J**, **a–f**, and **α–γ**) ESI mass spectra of the intermediates formed during the degradation of the CV dye after they were separated by HPLC method.

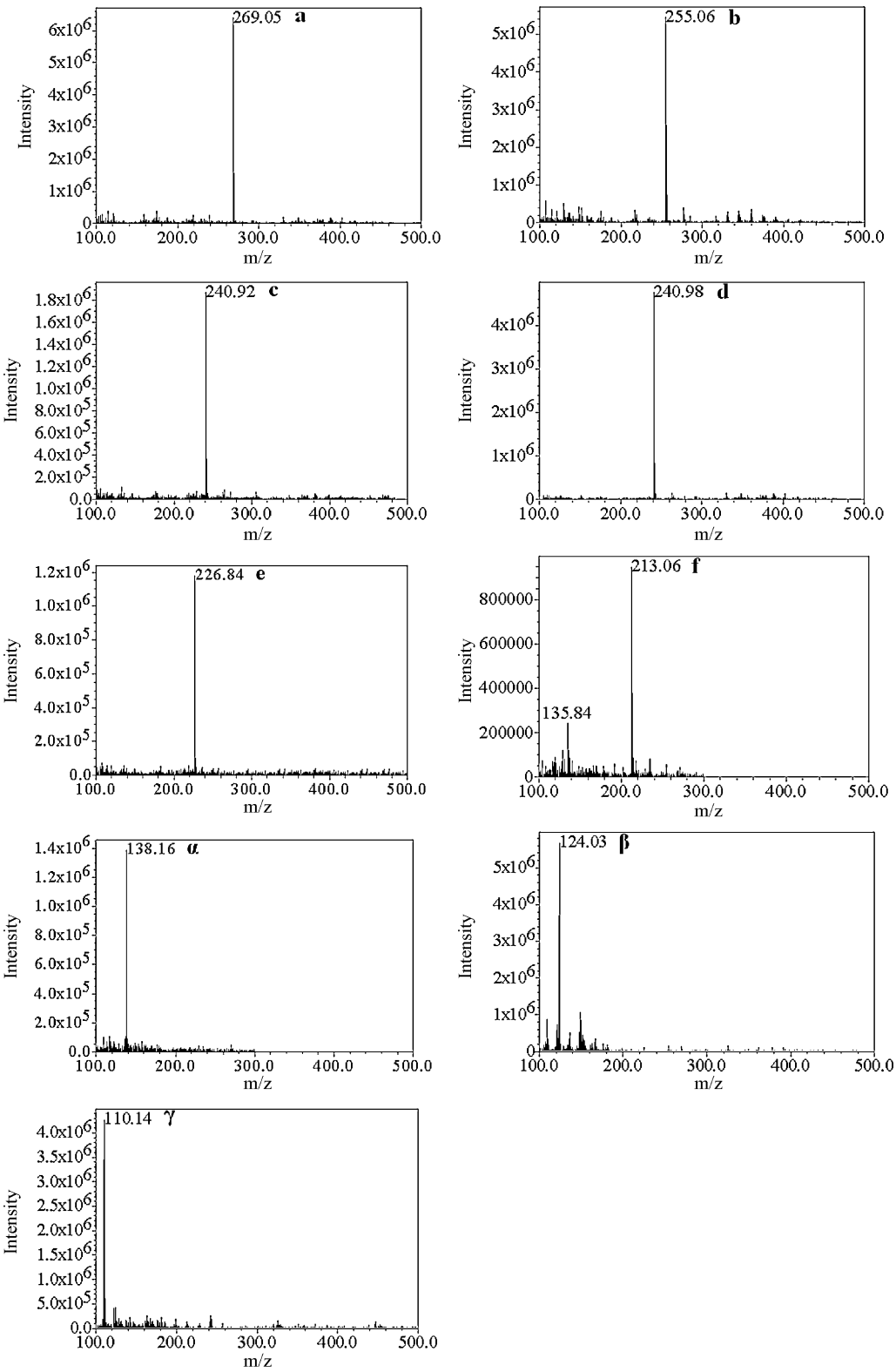

Fig. 10. (*Continued*).

The data show that absorption spectral bands shift hypsochromically from 588.2 to 543.4 nm (Fig. 5a, spectrum **A**–**J**), 376.4 to 337.5 nm (Fig. 5(b), Spectrum **a**–**f**), and 309.7 to 278.1 nm (Fig. 5(c), Spectrum **α**–**γ**). As can be seen, the 19 compounds can be distributed into three different aromatic groups: (i) intermediates of *N*-de-methylation of *N*,*N*,*N*′,*N*′,*N*″,*N*″-hexaethylpararosaniline (CV; **A**), (ii) intermediates of *N*-de-methylation of 4-(*N*,*N*-dimethylamino)-4′-(*N*′,*N*′-dimethylamino)benzophenone (**a**), and (iii) intermediates of *N*-de-methylation of 4-(*N*,*N*-dimethylamino)phenol (**α**), respectively. This hypsochromic shift of the absorption band was possible due to the formation of series of *N*-de-methylated intermediates in a stepwise manner. For example, λ_{max} of **A**, **B**, **C**, **D**, **E**, **F**, **G**, **H**, **I**,

and **J** are 588.2, 581.1, 573.4, 579.5, 566.7, 570.1, 561.8, 566.2, 554.1 and 543.4 nm; λ_{max} of **a**, **b**, **c**, **e**, **e**, and **f** are 376.4, 366.4, 364.4, 358.8, 357.3, and 337.5 nm; and **α**, **β**, and **γ** are 309.7, 283.6, and 278.1 nm, respectively. Given the identification of *N*-dimethylated aromatic amines in groups such as **A–J**, **a–f**, and **α–γ**, this was also done for the Fenton-like oxidation of CV dye (Fig. 9). Similar phenomena were observed during the photocatalytic degradation of sulforhodamine-B [49], rhodamine-B [50], and acid blue 1 [51]. The wavelength shift depicted in Figs. 8 and 9 is caused by the *N*-de-methylation of CV because of the attack by one of the •OH radicals on the *N*,*N*-dimethyl group.

Correspondingly, the *N*-de-methylated intermediates of Fenton and Fenton-like reactions are further identified using the HPLC–ESI mass spectrometric method due to a similar situation in the intermediates category. Therefore, we have used the higher removal rate of the Fenton system to identify intermediates by HPLC–ESI mass spectrometry.

3.3.2. LC–MS determination

The *N*-de-methylated intermediates were further identified using the HPLC–ESI mass spectrometric method. The molecular ion peaks appeared in the acid forms of the intermediates. As shown in Fig. 10, the mass spectral analysis confirmed the components **A** (m/z = 372.18), **B** (m/z = 358.14), **C** (m/z = 344.10), **D** (m/z = 344.09), **E** (m/z = 330.10), **F** (m/z = 330.36), **G** (m/z = 316.11), **H** (m/z = 316.11), **I** (m/z = 302.06), **J** (m/z = 288.07), **a** (m/z = 269.05), **b** (m/z = 255.06), **c** (m/z = 240.92), **d** (m/z = 240.98), **e** (m/z = 226.84), **f** (m/z = 213.06), **α** (m/z = 138.16), **β** (m/z = 124.03), and **γ** (m/z = 110.14). These species correspond to three pairs of isomeric molecules with two to four less methyl groups than CV. For example, **B** is formed by removal of a methyl group from two different sides of the CV molecule while the other corresponding isomer in this pair, **D**, is produced by removal of two methyl groups from the same side of the CV structure. In the second pair of isomers, **E** is formed by removal of three methyl groups from each side of the CV molecule while the other isomer in this pair, **F**, is produced by removal of two methyl groups from one side of the CV structure while one more methyl group was removed from the other side of the CV structure. In the third pair of isomers, **H** is formed by removal of two methyl groups from two different sides of the CV molecule while the other isomer in this pair, **G**, is produced by removal of two methyl groups from the same side of the CV structure and by removal of a methyl group from the remaining two sides of the CV structure. Because the polarities of the **D**, **F** and **H** species are greater than those of the **C**, **E** and **G** intermediates, the latter were eluted after the **D**, **F** and **H** species, respectively. Since two *N*-methyl groups are stronger auxochromic moieties than the *N*,*N*-dimethyl groups and amino group, the maximal absorption of the **D**, **F** and **H** intermediates was anticipated to occur at wavelengths longer than the band position of the **C**, **E** and **G** species, respectively (Table 1). On the other hand, the oxidation process is initiated by hydroxylation of the central carbon of CV. For example, the intermediates 4-(*N*,*N*-dimethylamino)-4′-(*N*′,*N*′-dimethylamino)benzo-phenone (**a**) and 4-(*N*,*N*-dimethylamino)phenol (**α**) are formed by an •OH radical attack on the conjugated structure, yielding a carbon-centered radical, which is subsequently attacked by molecular oxygen, leading to cleavage of the CV conjugated chromophore structure. Afterwards, compounds **a** and **α** were possibly formed by a series of *N*-de-methylated intermediates in a stepwise manner. This was also reported for the electro-Fenton [52], and photo-Fenton [53] treatment of malachite green, as well as for the photocatalysis of Basic Violet 4 [54]. During the initial period of the Fenton oxidation of CV, competitive reactions between *N*-de-methylation and cleavage of the CV chromophore ring structure occur, with *N*-de-methylation predominating as illustrated in Fig. 11. The *N*-de-methylated intermediates (**A–J**) observed are shown in Fig. 11(a) (curve A–J), and

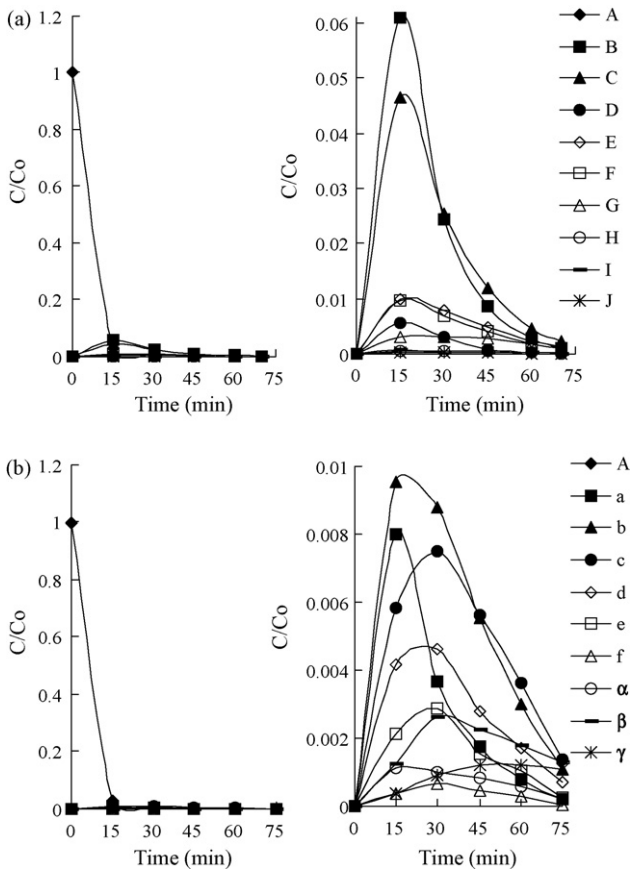

Fig. 11. Variations in the relative distribution of the intermediates products obtained from the degradation of CV as a function of reaction time. Reaction conditions: $[CV]_o$ = 0.15 mM, pH 3; (a) compounds **A–J**, (b) compounds **a–f**, and **α–γ**.

they reached a maximum concentration after a 15-min reaction period. Meanwhile, cleavage of the CV chromophore intermediates (**a–f** and **α–γ**) were observed to reach maximum concentrations after 15–45 min (Fig. 11(b)). The analysis results showed that **A–J** reached the maximal concentration faster than **a–f** or **α–γ**. Therefore, the conclusion drawn above should be that *N*-de-methylation is favored over cleavage of the CV chromophore ring structure. These phenomena indicate that the *N*-de-methylation process predominates and that the cleavage of the conjugated structure occurs at a somewhat slower rate.

3.3.3. GC–MS determination

The intermediates arise from the degradation of *N*,*N*,*N*′,*N*′,*N*″,*N*″-hexaethylpararosaniline (CV) and include compounds **B–J**, **a–f**, and **α–γ**, which were found for the first time in the Fenton (Fe^{2+}/H_2O_2) process. Earlier reports [37] failed to identify the *N*-de-methylated intermediates formed in the photocatalytic degradation of CV through GC–MS analysis. The volatilities of these intermediates are likely too small to be eluted out under the gas chromatographic conditions used, and the polarity is so great that they were eluted with the solvent phase in our HPLC analysis. Therefore, the intermediates were also performed by solid-phase extraction followed by GC–MS analysis. SPE has been demonstrated to be more efficient than traditional liquid–liquid extraction (LLE) in the analysis of water samples containing very polar intermediates resulting from the photocatalytic degradation process [55]. Fig. 7 shows the GC–MS chromatogram obtained for a SPE extract of CV solution after 60 min of Fenton reaction. Blank analysis helped us to discard those peaks coming from the sample handling procedure and chromatographic sys-

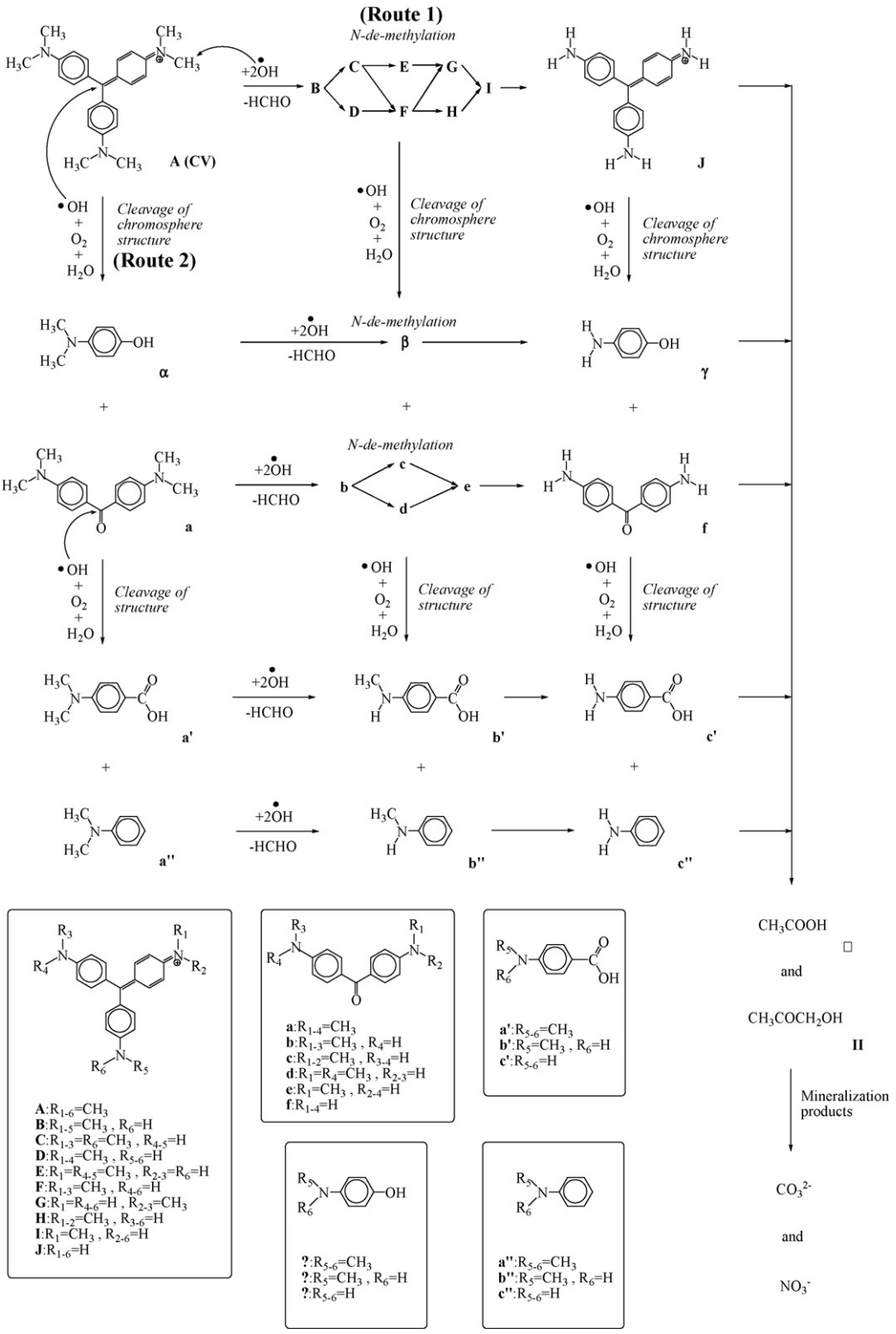

Scheme 1. Proposed degradation mechanism of CV under Fenton (or Fenton-like) processes followed by the identification of several intermediates by HPLC–ESI and GC–EI mass spectral techniques.

tem. The GC–MS analysis of the Fenton process of CV solution showed the formation of final intermediate products. Four of these intermediates have been identified using an identification program of the NIST library with a fit value higher than 80% in all cases. Analyses by GC/MS led to the identification of these compounds (**b**″, **c**″, **I** and **II**) which did not possess the bis-aminobenzophenone group. The mass spectra of these intermediates are shown in Fig. 7. The peaks eluting at 32.48 min, 30.39 min, 12.64 min, and 9.39 min during GC/MS were identified as *N*-methylaminobenzene (**b**″), aminobenzene (**c**″), 1-hydroxy-2-propanone (**I**), and acetic acid (**II**) with fit values of 92%, 83%, 97% and 97%, respectively, found by searching the mass spec-

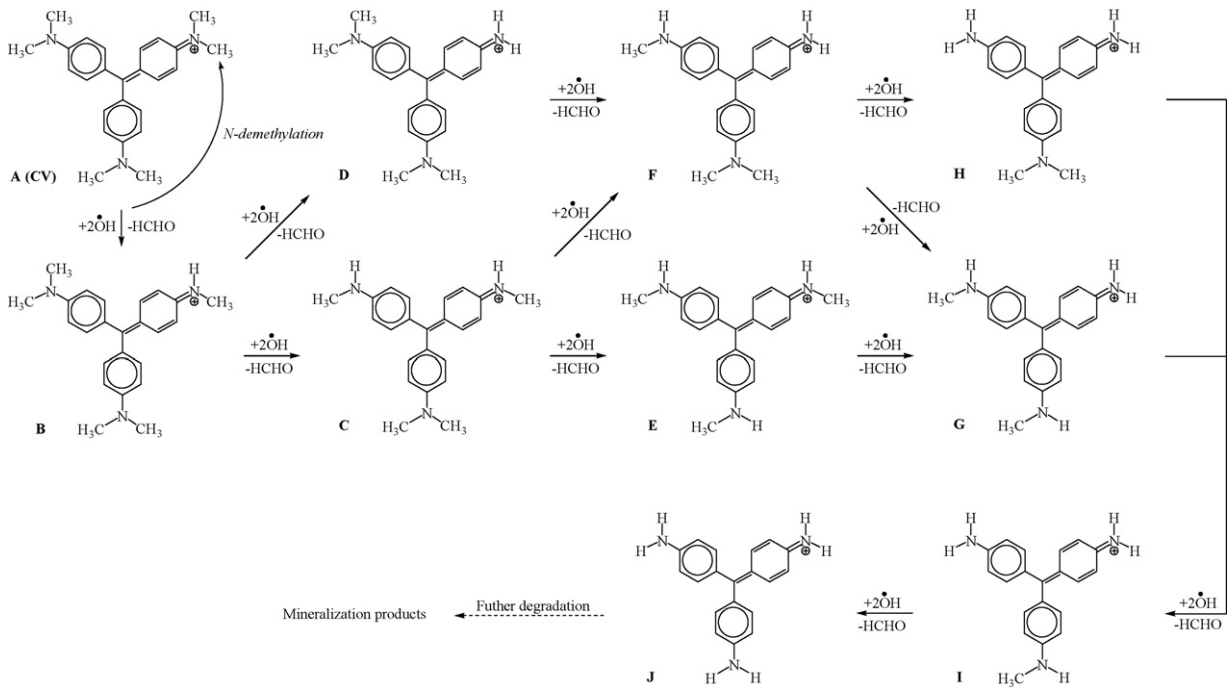

Scheme 2. Proposed *N*-de-methylation mechanism of CV under the Fenton process.

tra library (Table 1). The former intermediates (compounds **b**″, **c**″) are the results of the cleavage of **a** and *N*-de-methylated **a** species, leading to *N*-methylaminobenzene and aminobenzene. A similar observation was made in the previous study [37], in which *p*-aminobenzoic acid and *N*-methylaminobenzene were detected as intermediates. The findings confirm the work of other authors. These results are consistent with some given by Muneer [56]. The latter intermediates consist of compounds **I**–**II** formed by cleavage of the aromatic derivatives, leading to aliphatic products.

3.4. Degradation pathways of CV

Based on the LC/MS and GC/MS analyses of the various Fenton/CV process intermediates, the degradation pathways for CV are proposed in Scheme 1. It involves two different pathways (Routes 1 and 2, respectively), corresponding to the two possible sites for the attack by •OH radicals on the CV molecule. As most of the •OH are generated directly from the reaction between the Fe^{2+} with H_2O_2, the species •OH is shown as the main oxidant though the parallel action of less oxidizing agents like HO_2• and H_2O_2 is not

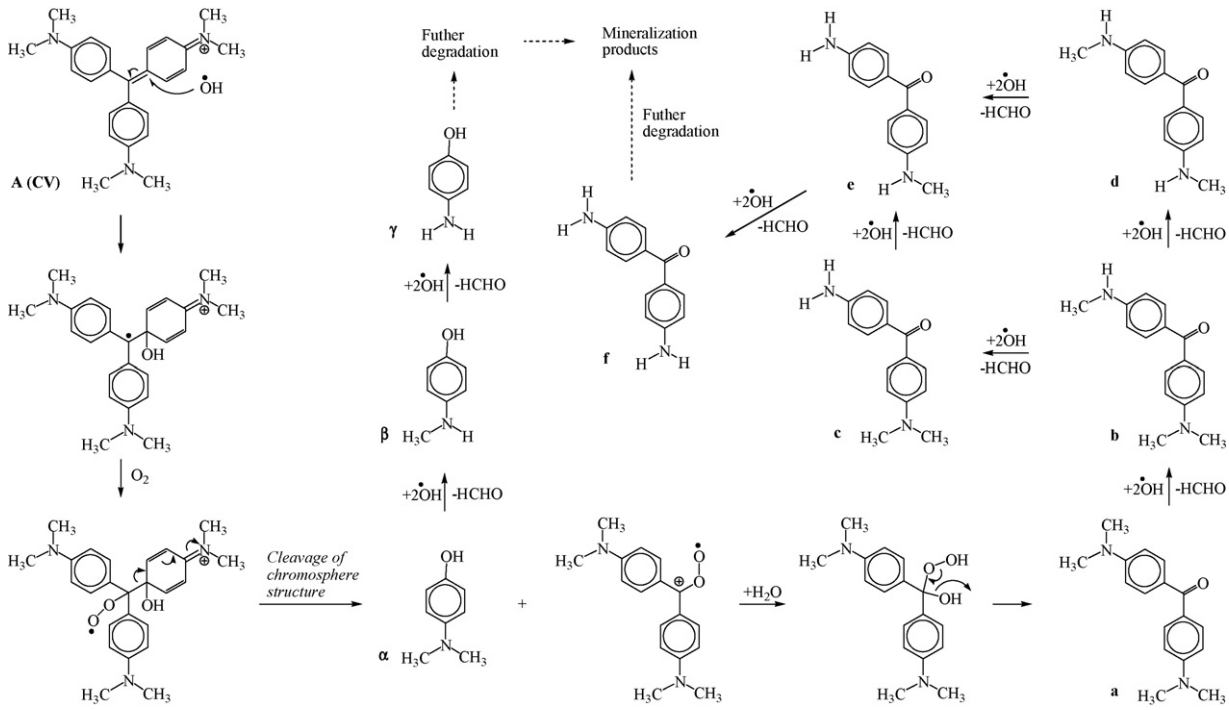

Scheme 3. Proposed mechanism of cleavage of chromosphere structure of CV under the Fenton process.

discounted. The *N*-de-methylation of CV occurs mostly through attack by •OH species on the *N*,*N*-dimethyl groups of CV, as shown in Scheme 2 (Route 1). The compound **B** is attacked by •OH radicals on the methyl group, and the formation of hydroxymethylated intermediates [38] which are themselves subsequently attacked by •OH radicals leads ultimately to *N*-de-methylation. The mono-de-methylated dye, **B** intermediates, can also be attacked by •OH radicals on the methyl group, and then the hydroxymethylation and *N*-de-methylation process described above continues until formation of the completely *N*-de-methylated dye, **F** intermediates. In addition to the *N*-de-methylation degradation route, an alternative pathway was also identified. A plausible mechanism for the formation of degradation products **a–f** and **α–γ** involving reaction with •OH radicals formed in the Fenton process is proposed in Scheme 3 (Route 2). The •OH radical attack on the conjugated structure yields a carbon-centered radical, which is subsequently attacked by molecular oxygen to lead ultimately to the formation of 4-(*N*,*N*-dimethylamino)-4′-(*N*′, *N*′-dimethylamino)benzophenone (**a**) and 4-(*N*,*N*-dimethylamino)phenol (**α**). Additionally, the species **a** can also be implicated in other similar events (cleavage of **a** chromophore structure) to yield *N*-methylaminobenzene (**b**″) and aminobenzene (**c**″). This is in agreement with mechanisms proposed by Muneer et al. for gentian violet [37]. It is known from previous photocatalytic studies that, after the formation of various aromatic derivatives, cleavage of the benzene or other organic rings takes place, and different aliphatic products are subsequently formed before complete mineralization [46]. Even though further oxidation leads to the ring-opening and the formation of aliphatic oxidation products (compounds **a**′–**c**′, and **a**″), these species will not be discussed here.

4. Conclusion

Knowledge of reaction pathways and transformation rates is critical for optimizing hazardous waste treatment and evaluating its effectiveness. In this study, we showed that optimum FR treatment was achieved with 1:100 (1:50) molar ratios of Fe^{2+} and H_2O_2 (Fe^{3+} and H_2O_2) at pH 3. CV, which was degraded in 30 min at pH 5, produced two set products. *N*-de-methylation and cleavage of the conjugated chromophore structure were the two major primary mechanisms of CV degradation by FR.

Acknowledgements

This research was supported by the National Science Council of the Republic of China (NSC 97-2113-M-142-002-MY2).

References

[1] H.J.H. Fenton, Oxidation of tartaric acid in the presence of iron, J. Chem. Soc. 65 (1894) 899–910.
[2] S.F. Kang, T.H. Wang, Y.H. Lin, Decolorization and degradation of 2,4-dinitrophenol by Fenton's reagent, J. Environ. Sci. Health A 34 (1999) 935–950.
[3] S.M. Kim, A. Vogelpohl, Degradation of organic pollutants by the photo-Fenton-process, Chem. Eng. Technol. 21 (1998) 187–191.
[4] H. Gulyas, Processes for the removal of recalcitrant organics from industrial wastewaters, Water Sci. Technol. 36 (1997) 9–16.
[5] S.F. Kang, C.H. Liao, H.P. Hung, Decolorization of textile wastewater by photo-Fenton oxidation technology, Chemosphere 41 (2000) 1287–1297.
[6] W.Z. Tang, R.Z. Chen, Decolorization kinetics and mechanisms of commercial dyes by H_2O_2/iron powder system, Chemosphere 32 (1996) 947–958.
[7] E.G. Solozhenko, N.M. Soboleva, V.V. Goncharuk, Decolourization of azo dye solution by Fenton's oxidation, Water Res. 29 (1995) 2206–2210.
[8] F. Chen, W. Ma, J. He, J. Zhao, Fenton degradation of malachite green catalyzed by aromatic additives, J. Phys. Chem. A 106 (2002) 9485–9490.
[9] B. Ensing, E.J. Baerends, Reaction path sampling of the reaction between iron(II) and hydrogen peroxide in aqueous solution, J. Phys. Chem. A 106 (2002) 7902–7910.
[10] J.A. Zazo, J.A. Casas, F. Mohedanoa, M.A. Gilarranz, A.J. Rodriaguez, Chemical pathway and kinetics of phenol oxidation by Fenton's reagent, Environ. Sci. Technol. 39 (2005) 9295–9302.
[11] C. Walling, Intermediates in the reactions of Fenton type reagents, Acc. Chem. Res. 31 (1998) 155–157.
[12] S.M. Scott, W.J. Hickey, R.F. Harris, Degradation of atrazine by Fenton's reagent: condition optimization and product quantification, Environ. Sci. Technol. 29 (1995) 2083–2089.
[13] P.K. Malik, Oxidation of safraine T in aqueous solution using Fenton's reagent: investment of an Fe (III) chelate in the catalytic hydroxygen peroxide oxidation of safraine T, J. Phys. Chem. A 108 (2004) 2675–2681.
[14] A. Masarwa, S. Rachmilovich-Calis, N. Meyerstein, Oxidation of organic substrates in aerated aqueous solutions by the Fenton reagent, Coord. Chem. Rev. 249 (2005) 1937–1943.
[15] J. Ma, W. Song, C. Chen, W. Ma, J. Zhao, Y. Tang, Fenton degradation of organic compounds promoted by dyes under visible irradiation, Environ. Sci. Technol. 39 (2005) 5810–5815.
[16] J.H. Sun, S.P. Sun, G.L. Wang, L.P. Qiao, Degradation of azo dye Amido black 10B in aqueous solution by Fenton oxidation process, Dyes Pigm. 74 (2007) 647–652.
[17] C. Walling, A. Goosen, Mechanism for the ferric ion catalyzed decomposition of hydrogen peroxide. Effect of organic substrates, J. Am. Chem. Soc. 95 (1973) 2987–2991.
[18] G.V. Buxton, C.L. Greenstock, W.P. Helman, A.B. Ross, Critical review of rate constants for reactions of hydrated electrons, hydrogen atoms and hydroxyl radicals in aqueous solution, J. Phys. Chem. Ref. Data 17 (1988) 513–886.
[19] W.G. Barb, J.H. Baxendale, P. George, K.R. Hargrave, Reactions of ferrous and ferric ions with hydrogen peroxide. Part I-the ferrous ion reaction, Trans. Faraday Soc. 47 (1951) 462–500.
[20] J.D. Laat, H. Gallard, Catalytic decomposition of hydrogen peroxide by Fe(III) in homogeneous aqueous solution: mechanism and kinetic modeling, Environ. Sci. Technol. 33 (1999) 2726–2732.
[21] S.S. Lin, M.D. Gurol, Catalytic decomposition of hydrogen peroxide on iron oxide: kinetics, mechanisms, and implications, Environ. Sci. Technol. 32 (1998) 1417–1423.
[22] C. Walling, K. Amarnath, Oxidation of mandelic acid by Fenton's reagent, J. Am. Chem. Soc. 104 (1982) 1185–1189.
[23] D.A. Wink, R.W. Nims, M.F. Desresters, P.C. Ford, L.K. Keefer, A kinetic investigation of intermediates formed during the Fenton reagent mediated degradation of N-nitrosodimethylamine: evidence for an oxidative pathway not involving hydroxyl radical, Chem. Res. Toxicol. 4 (1991) 510–512.
[24] Y. Dong, H. Fujii, M.P. Hendrich, R.A. Leising, G. Pan, C.R. Randall, E.C. Wilkinson, Y. Zang, L. Que Jr., B.G. Fax, K. Kauffmann, E. Muck, A high-valent nonheme iron intermediate. structure and properties of $[Fe_2(\mu\text{-}O)_2(5\text{-Me-TPA})_2](ClO_4)_3$, J. Am. Chem. Soc. 117 (1995) 2778–2792.
[25] R.A. Arasasingham, C.R. Cornman, A.L. Balch, J. Am. Chem. Soc. 111 (1989) 7800–7805.
[26] D.T. Sawyer, A. Sobkowiak, T. Matsushita, Metal [ML_x; M = Fe, Cu, Co, Mn]/hydroperoxide-induced activation of dioxygen for the oxygenation of hydrocarbons: oxygenated Fenton chemistry, Acc. Chem. Res. 29 (1996) 409–416.
[27] I. Ymazaki, L.H. Piette, EPR spin trapping study on the oxidizing species formed in the reaction of the ferrous ion with hydrogen peroxide, J. Am. Chem. Soc. 113 (1991) 7588–7593.
[28] M.L. Kremer, Complex versus 'Free Radical' mechanism for the catalytic decomposition of H_2O_2 by Fe^{3+}, Int. J. Chem. Kinet. 17 (1985) 1299–1314.
[29] B. Ensing, F. Buda, E.J. Baerends, Fenton-like chemistry in water: oxidation catalysis by Fe(III) and H_2O_2, J. Phys. Chem. A 107 (2003) 5722–5731.
[30] D.A. Wink, R.W. Nims, J.E. Saavedra, W.E. Utermahlen, P.C. Ford, The Fenton oxidation mechanism: reactivities of biologically relevant substrates with two oxidizing intermediates differ from those predicted for the hydroxyl radical, Proc. Natl. Acad. Sci. U.S.A. 91 (1994) 6604.
[31] L. Young, J. Yu, Ligninase-catalysed decolorization of systhetic dyes, Water Res. 31 (1997) 1187–1193.
[32] Ullmann's Encyclopedia of Industrial Chemistry, Part A27. Triarylmethane and Diarylmethane Dyes, 6th ed., Wiley-VCH, New York, 2001.
[33] R. Docampo, R.P.A. Muniz, F.S. Cruz, R.P. Mason, Light-enhanced free radical formation and trypanocidal action of gentian violet, Science 200 (1983) 1292.
[34] G.L. Indig, G.S. Anderson, M.G. Nichol, J.A. Bartlett, W.S. Mellon, F. Sieber, Effect of molecular structure on the performance of triarylmethane dyes as therapeutic agents for photochemical purging of autologous bone marrow grafts from residual tumor cells, J. Pharm. Sci. 89 (2000) 88–99.
[35] B.P. Cho, T. Yang, L.R. Blankenship, J.D. Moody, M. Churchwell, F.A. Bebland, S.J. Culp, Synthesis and characterization of *N*-demethylated metabolites of Malachite Green and Leucomalachite Green, Chem. Res. Toxicol. 16 (2003) 285–294.
[36] A.C. Bhasikuttan, A.V. Sapre, L.V. Shastri, Photoinduced electron transfer in crystal violet (CV^+)–bovine serum albumin (BSA) system: evaluation of reaction paths and radical intermediates, J. Photochem. Photobiol. A: Chem. 150 (2002) 59–66.
[37] M. Saquib, M. Muneer, TiO_2-mediated photocatalytic degradation of a triphenylmethane dye (gentian violet), in aqueous suspensions, Dyes Pigm. 56 (2003) 37–49.
[38] C.C. Chen, F.D. Mai, K.T. Chen, C.S. Lu, Photocatalyzed *N*-de-methylation and degradation of crystal violet in titania dispersions under UV irradiation, Dyes Pigm. 75 (2007) 434–442.

[39] S.R. Couto, A. Dominguez, A. Sanroman, Photocatalytic degradation of dyes in aqueous solution operating in a fluidized bed reactor, Chemosphere 46 (2002) 83–86.
[40] F.A. Alshamsi, A.S. Albadwawi, M.M. Alnuaimi, M.A. Rauf, S.S. Ashraf, Comparative efficiencies of the degradation of Crystal Violet using UV/hydrogen peroxide and Fenton's reagent, Dyes Pigm. 74 (2007) 283–287.
[41] I. Sirés, E. Guivarch, N. Oturan, M.A. Oturan, Efficient removal of triphenylmethane dyes from aqueous medium by in situ electrogenerated Fenton's reagent at carbon-felt cathode, Chemosphere 72 (2008) 592–600.
[42] E.M. Siedlecka, W. Mrozik, Z. Kaczynski, P. Stepnowski, Degradation of 1-butyl-3-methylimidazolium chloride ionic liquid in a Fenton-like system, J. Hazard. Mater. 154 (2008) 893–900.
[43] Y. Sun, J.J. Pignatello, Photochemical reactions involoved in the total minerization of 2,4-D by Fe^{3+}/H_2O_2/UV, J. Environ. Qual. 27 (1993) 304–310.
[44] J.L. Allen, J.R. Meinertz, Post-column reaction for simultaneous analysis of chromatic and leuco forms of malachite green and crystal violet by high-performance liquid chromatography with photometric detection, J. Chromatogr. A 536 (1991) 217–222.
[45] M.C. Lu, J.N. Chen, C.P. Chang, Oxidation of dichlorvos with hydrogen peroxide using ferrous ion as catalyst, J. Hazard. Mater. 69 (1999) 277–288.
[46] H. Gallard, J. De Laat, B. Legube, Spectrophotometric study of the formation of iron(III)-hydroperoxy complexes in homogeneous aqueous solutions, Water Res. 33 (1999) 2929–2936.
[47] J.J. Pignatello, Dark and photoassisted Fe^{3+}-catalysed degradation of chlorophenoxy herbicides by hydrogen peroxide, Environ. Sci. Technol. 26 (1992) 944–951.
[48] W.Z. Tang, C.P. Huang, 2,4-dichlorophenol oxidation kinetics by Fenton's reagent, Environ. Technol. 17 (1996) 1371–1378.
[49] C.C. Chen, W. Zhao, J.G. Li, J.C. Zhao, H. Hidaka, N. Serpone, Formation and identification of intermediates in the visible-light-assisted photodegradation of sulforhodamine-B dye in aqueous TiO_2 dispersion, Environ. Sci. Technol. 36 (2002) 3604–3611.
[50] T. Wu, G. Liu, J. Zhao, H. Hidaka, N. Serpone, Photoassisted degradation of dye pollutants. v. self-photosensitized oxidative transformation of rhodamine B under visible light irradiation in aqueous TiO_2 dispersions, J. Phys. Chem. B 102 (1998) 5845–5851.
[51] C.C. Chen, H.J. Fan, J.L. Jan, Degradation pathways and efficiencies of acid blue 1 by photocatalytic reaction with ZnO nanopowder, J. Phys. Chem. C 112 (2008) 11962–11972.
[52] M.A. Oturan, E. Guivarch, N. Oturan, I. Sirés, Oxidation pathways of malachite green by Fe^{3+}-catalyzed electro-Fenton process, Appl. Catal. B: Environ. 82 (2008) 244–254.
[53] F. Chen, J. He, J. Zhao, J.C. Yub, Photo-Fenton degradation of malachite green catalyzed by aromatic compounds under visible light irradiation, New J. Chem. 26 (2002) 336–341.
[54] C.C. Chen, C.S. Lu, Photocatalytic degradation of basic violet 4: degradation efficiency, product distribution, and mechanisms, J. Phys. Chem. C111 (2007) 13922–13932.
[55] A.R. Fernandez-Alba, A. Aguera, M. Contreras, G. Penuela, I. Ferrer, D. Barcelo, Comparison of various sample handling and analytical procedures for the monitoring of pesticides and metabolites in ground waters, J. Chromatogr. A 823 (1998) 35–47.
[56] J. Lee, W. Choi, Effect of platinum deposits on TiO_2 on the anoxic photocatalytic degradation pathways of alkylamines in water: dealkylation, Environ. Sci. Technol. 38 (2004) 4026–4033.